

Article

MicroRNA Sequencing Reveals the Effect of Different Levels of Non-Fibrous Carbohydrate/Neutral Detergent Fiber on Rumen Development in Calves

Mingming Xue [†], Kejun Wang [†] , Ansi Wang, Ruiting Li, Yadong Wang, Shuaijie Sun, Duo Yan, Guohua Song, Huifen Xu, Guirong Sun ^{*} and Ming Li ^{*}

College of Animal Science and Veterinary Medicine, Henan Agricultural University, Zhengzhou 450046, China

^{*} Correspondence: 13803849306@163.com (M.L.); grsun2000@126.com (G.S.); Tel.: +86-0371-56990218 (M.L.)

[†] These authors contributed equally to this paper.

Received: 26 April 2019; Accepted: 26 July 2019; Published: 28 July 2019



Simple Summary: By histological sectioning and staining of rumen tissues from calves fed with a high or low ratio of non-fibrous carbohydrate/neutral detergent fiber diet, we found that the length and width of papillae were significantly affected by the ratio. From microRNA expression analysis we found cell proliferation, differentiation, physical and nutrient stimuli processes participate in the development of the rumen. In addition, bta-miR-128 was found to affect rumen development by negatively regulating *PPARG* and *SLC16A1*. Our findings provided an important resource for the continuing study of rumen development and absorption.

Abstract: Rumen development in calves is affected by many factors, including dietary composition. MicroRNAs (miRNAs) are known to function in the development of the rumen in cattle, what is not known is how these miRNAs function in rumen development of calves fed with high and low ratios of non-fibrous carbohydrate (NFC)/neutral detergent fiber (NDF). A total of six healthy Charolais hybrids bull calves of similar weight were divided into two groups; three calves were fed a mixed diet with NFC/NDF = 1.35 (H group), and three were fed a mixed diet with NFC/NDF = 0.80 (L group). After 105 days on the diet, calves were sacrificed and rumen tissues were collected. Tissues were subjected to histological observation and miRNA expression analysis. Functional enrichment analysis was conducted on the target genes of the miRNAs. Targeting and regulatory relationships were verified by luciferase reporter assay and quantitative PCR (qPCR). We found that the length of rumen papilla in the L group was significantly greater than that in the H group, while the width of rumen papilla in H group was significantly greater than that that in L group. We identified 896 miRNAs; 540 known miRNAs, and 356 novel predicted miRNAs. After statistical testing, we identified 24 differentially expressed miRNAs (DEmiRNAs). miRNA-mRNA-cluster network analysis and literature reviews revealed that cell proliferation, differentiation, physical and nutrient stimuli processes participate in rumen development under different NFC/NDF levels. The regulatory relationships between three DEmiRNAs and five target genes were verified by examining the levels of expression. The binding sites on bta-miR-128 for the peroxisome proliferator activated receptor gamma (*PPARG*) and solute carrier family 16 member 1 (*SLC16A1*) genes were investigated using a dual luciferase assay. The results of this study provide insight into the role of miRNAs in rumen development in calves under different NFC/NDF levels.

Keywords: calf; rumen; papilla; miRNA

1. Introduction

The rumen is the primary site for fermentation in ruminant animals as well as an important site for nutrient absorption, digestion, and metabolism. Digestion and metabolism mainly involve the degradation of fiber and the absorption of volatile fatty acids by the rumen epithelium. Rumen epithelial morphology and development is affected by the feed quality and particle size [1,2] which obviously has an affect on the animal health and growth. Several publications have suggested that miRNAs play a crucial role in regulating the rumen development during bovine embryonic development [3–6]. However, the effect of different NFC/NDF levels on miRNAs involved in the rumen development process in calves is unclear.

MiRNAs are a class of non-coding single-stranded RNA molecules, approximately 22 nucleotides (nt) in length, that are involved in post-transcriptional regulation of gene expression in plants and animals, including early development [7], cell proliferation, apoptosis, cell death [8], cell differentiation [9], and fat metabolism [10]. In broad terms miRNAs degrade their target mRNA or inhibit its translation, although they function in many other ways as well [11], such as pri-miRNAs coding for peptides [12], interacting with non-Ago proteins [13], activating Toll-like receptors [14], upregulating protein expression, directing transcription, targeting mitochondrial transcripts or nuclear ncRNAs [15]. MiRNAs play a wide role in the life's processes.

The aim at this study is to investigate the effect of different NFC/NDF levels on the miRNAs participating in rumen development in calves. Rumen tissue was observed by histological sectioning and staining, and high-throughput sequencing was used to identify the miRNAs that affect the rumen development. In addition, the network of regulatory relationships between components of the miRNA-mRNA-cluster network was elucidated by analyzing DE miRNAs, target genes, and clusters of interest.

2. Materials and Methods

2.1. Animals and Experimental Design

2.1.1. Ethics Statement

All experiments and animal care procedures were performed in accordance with the protocols and guidelines approved by the Institutional Animal Care and Use Committee (IACUC) of Henan Agriculture University (Zhengzhou, China) (Permit Number: 11-0085; Date: 06-2011).

2.1.2. Experimental Animals and RNA Isolation

Six Charolais hybrid bull calves were used in our study; all calves were raised in the same environmental conditions. Three calves were fed total mixed rations with an NFC/NDF ratio of 1.35 (H group), and three calves were fed total mixed rations with an NFC/NDF ratio of 0.80 (L group). The calves were fed according to the “Chinese Beef cattle Raising Standard” (2004). “Dietary nutrition level (dry basis)” is published in [16]. NDF content in the feed samples was based on the observations by Van Soest [17]. The experiment lasted 105 days, a pre-trial period was 15 days and the trial period was 90 days. Calves were slaughtered at the end of the test. The ventral sac of the rumen was chosen for study because it is the site with the highest capillary blood flow per unit weight mucosa [18]. Rumen tissues were harvested with silver paper then either frozen immediately in liquid nitrogen and stored at -80°C or prepared for histological sectioning.

2.1.3. Preparation and Observation of Rumen Sections

Rumens were exteriorized and separated as described in Carstens et al. [19]. Rumen tissue was cut into 2 cm² sections with sterile surgical scissors, washed several times in pre-cooled PBS buffer (pH = 7.2), then fixed overnight in 4% paraformaldehyde. Tissue was then dehydrated, cleared, and embedded in paraffin. Samples were cut into 6 μm sections then stained with hematoxylin and

eosin (HE) using the standard protocol. The morphological characteristics of the rumen papilla were observed with light microscopy. The papillae length, width, and tunica muscularis were measured five times using Motic images advanced 3.2 software.

2.2. MicroRNA Sequencing

2.2.1. miRNA library Construction and Illumina Deep Sequencing

A total of four miRNA libraries were constructed from two rumen tissues per group, using the Illumina® small RNA Library Prep Set (NEB, Ipswich, MA, USA) according to the manufacturer's protocol. Briefly, 1.5 µg of RNA per sample was brought to 6 µL with H₂O and adapters were ligated to the 3' and 5' ends. These products were used for reverse transcription and amplification. The amplicons were purified by agarose gel separation. The RNA libraries were quantitated using a Qubit 2.0 fluorometer (Life Technologies, Camarillo, CA, USA) and brought to 1 ng/µL. RNA quality was analyzed using an Agilent Bioanalyzer 2100 (Agilent, Santa Clara, CA, USA). The RNA integrity number (RIN) was more than 8. The effective concentration of the miRNA library was assessed using qPCR. The libraries were sequenced using an Illumina HiSeq 2500 system at Biomarker Technologies (Beijing, China).

2.2.2. Sequence Analyses

Raw reads were assessed for quality using the Illumina Pipeline filter (Solexa v0.3). The pipeline performed the following steps: (1) Reads were set aside if more than 20% of their nucleotides had quality scores of less than 30. (2) 3' adapter sequences were trimmed. (3) Reads were set aside if more than 10% of their nucleotides were unknown (N). (4) Reads shorter than 18 or longer than 30 nucleotides were removed. Each sample yielded more than 19.85 M clean reads. Bowtie v.1.1.0 was used to identify snRNAs, tRNAs, rRNAs, snoRNAs, various ncRNAs, and low-complexity sequences by comparing clean reads against the Repbase, GtRNADB, Rfam, and Silva databases. Bowtie was also used to map clean reads to the bovine reference genome (UMD_3.1.1). The reads were then compared with the known cattle pre-miRNAs and mature miRNAs in miRBase (v21) [20]. Novel miRNAs were predicted using miRDeep2 [21].

2.2.3. Differential Expression Analysis of miRNAs

To estimate miRNA levels in each sample, data were quantified as transcripts per million clean reads (TPM) to calculate and normalize expression [22]. Differential expression analysis was performed using DESeq R to compare the two groups [23]. MicroRNAs with adjusted $p \leq 0.05$ and $|\log_2(\text{fold change})| \geq 1$ were classified as DE miRNAs.

2.2.4. MiRNA Target Prediction, Functional Annotation, and Interaction Networks

Based on the miRNA sequences, MiRanda [24] and RNAhybrid [25] were used to predict DE miRNA target genes. Target genes that were recognized by both programs were retained. KOBAS [26] was used to test the statistical enrichment of the target genes in the gene ontology (GO) [27] and Kyoto encyclopedia of genes and genomes (KEGG) [28] databases. Interactions among the miRNAs and mRNAs were constructed and visualized as networks using Cytoscape [29].

2.3. Verification of Sequencing Results

2.3.1. Validation of Relative Expression of miRNAs and mRNAs

Seven differentially expressed miRNAs (DE miRNA) and six target genes were selected. The relative expression levels of five selected DE miRNAs were randomly validated for the reliability of the sequencing data. The relative expression levels of all of the DE miRNAs were analyzed by stem-loop quantitative real-time reverse transcription PCR. The predicted relationships between three DE miRNAs

and six target genes were tested. Target genes were validated by quantitative real-time reverse transcription PCR. Total RNA was extracted using TRIzol reagent then reversed transcribed using a PrimeScript RT reagent Kit with gDNA Eraser (TaKaRa). The Specific miRNA RT primers and seven pairs of qPCR primers were designed by RiboBio (RiboBio Co., Guangzhou, Guangdong, China). The mRNA primers (10 $\mu\text{mol}/\mu\text{L}$) were designed by Biosunya (Biosunya Biotechnology Co. Ltd., Shanghai, China); primers are listed in Supplementary Table S1. qPCR reactions were performed in triplicate using on a LightCycler 96 instrument (Roche, Indianapolis, IN, USA). The volume of each reaction was 10 μL : 5 μL of SYBR Premix Ex Taq II kit (TaKaRa), 1 μL of a mix of forward and reverse, 3 μL of RNase-free H_2O , and 1 μL of cDNA. Three common bovine housekeeping genes, glyceraldehyde-3-phosphate dehydrogenase (*GAPDH*), actin beta (*ACTB*), and beta-2-microglobulin (*B2M*) were tested for being used as internal controls. Since *GAPDH* had the lowest standard deviation (0.64, \pm Ct) and a lower coefficient of variation (3.2, %Ct), it was chosen as the internal control standard. U6 snRNA were chosen as the miRNA internal control [30–33]. The $2^{-\Delta\Delta\text{Ct}}$ method was used to determine the relative mRNA and miRNA abundance [34].

2.3.2. Vector Construction

The 3' untranslated region (UTR) of the *PPARG* gene, containing the bta-miR-128 binding site, was amplified by PCR using bovine genomic DNA as the template. The amplicon was purified then ligated into the XhoI–NotI site of the psiCHECKTM-2 vector. The resulting plasmid was used to transform *E. coli* DH5 α . Using “white-blue colony selection,” white colonies were cloned then amplified. The final recombinant plasmid was named *PPARG*-3'UTR-WT. The seed region of the bta-miR-128 binding site was mutated (Tsingke Company) and *PPARG*-3'UTR-Mut was constructed. The psiCHECKTM-2 reporter plasmid was a gift from Dr. Guirong Sun. Similarly, luciferase vectors of solute carrier family 16 member 1 were constructed (*SLC16A1*-3'UTR-WT and -Mut); *SLC16A1*-3'UTR-Mut was constructed using primer mutation. All plasmids were extracted using an EndoFree Mini Plasmid Kit II (TIANGEN, Beijing, China) and were sequenced by Biosunya Biotechnology Co. Ltd. (Shanghai, China). Primers are listed in Supplementary Table S1.

2.3.3. Cell Culture and Luciferase Reporter Assay

HEK293T [35] cells were maintained in high glucose medium supplemented with 10% fetal bovine serum (Biological Industries, Israel). A total of 5×10^5 cells/well were seeded into each well of a 6-well plate, when approximately 70% confluent, 100 ng of *PPARG*-UTR-WT, and *PPARG*-UTR-Mut were cotransfected with 20 nM negative control (NC) or bta-miR-128 mimic (GenePharma, Shanghai, China) using Lipofectamine 2000 (Solarbio, Beijing, China) according to the manufacturer's instructions. The medium was replaced after 6 h and the relative luciferase activity was measured after 48 h of using the Dual-Luciferase Reporter Assay System (Solarbio, Beijing, China) on a Fluoskan Ascent FL instrument (Thermo Fisher Scientific, Shanghai, China). *Renilla* luciferase (Rluc) activity was normalized to firefly luciferase activity. Relative luciferase activity was calculated to assess regulation of gene transcription in the treatment group. The experiment was performed using three replicates. Similarly, the target relationship between *SLC16A1* and bta-miR-128 was analyzed.

2.4. Statistical Analyses

Data were evaluated for differences by one-way ANOVA using SPSS 18.0 software (IBM, Chicago, IL, USA) * $p < 0.05$; ** $p < 0.01$. Data are expressed as the mean \pm standard error of the mean. Origin software (Northampton, MA, USA) and GraphPad Prism 5 software (San Diego, CA, USA) were used for graphics.

3. Results and Discussion

3.1. Effect of NFC/NDF Levels on Rumen Development of Calf

The rumen is a digestive organ unique to ruminant animals (sheep, cattle, goats, deer, giraffes, and llamas). The development of its epithelium, particularly the height of the papillae, greatly affects the digestive function [36,37]. Growth and development of rumen epithelium is influenced by numerous factors. Steele, M.A et al. have reported that dietary energy levels affect the morphological development of rumen epithelium, and a diet high in grain damages the epithelium in cattle [38]. In this study, Charolais hybrid bull calves were fed a high and low ratio of NFC/NDF, the H group was fed a ratio of NFC/NDF of 1.35, and L group was fed a ratio of NFC/NDF of 0.80. After 105 days, samples of the rumen tissue were collected. The evidence from HE staining revealed that papillae length in the H group was significantly shorter than that in the L group ($p < 0.05$); however, the papillae width of H group was significantly wider than in the L group ($p < 0.05$) (Figure 1A,B). We also observed no obvious difference in the thickness of the tunica muscularis between the groups. This result suggested that the level of NFC/NDF affects the development of papillae particularly their length and width. The molecular mechanism behind how NFC/NDF levels influence rumen development is not well understood, so to gain a better understanding, at the molecular level, of the effect of NFC/NDF levels in these calves, the miRNA profiles of the tissues were compared.

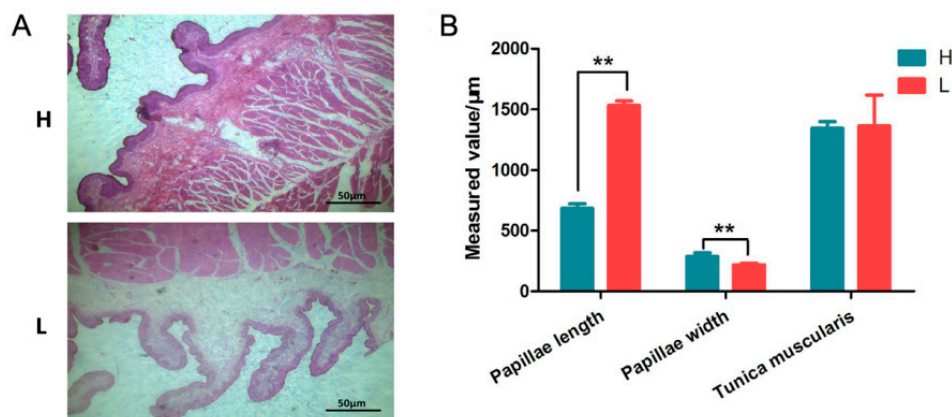


Figure 1. Histological observation of calf rumen tissues (n = 3). (A) Histological section of rumen tissues, H and L groups. (B) Quantification of papillae length and width, and the thickness of the tunica muscularis.

3.2. Overview of Small RNA Deep Sequencing Data

Using the Illumina HiSeq 2500 platform, four libraries from two groups were constructed and sequenced, yielding more than 1.48 million reads ranging in length from 18–30 nt (Table S2). Over 90% of the reads were retained after quality control and were analyzed to identify the candidate miRNAs (Table S2). A total of 896 miRNAs were found, of which 540 had been identified previously, and 356 were novel predicted miRNAs. The distribution of the lengths of the mature miRNAs is presented in Figure 2A. The most common length was 21–23 nt (Figure 2A), and the length distributions of the two groups appear to be identical (Figure 2B). These results suggest that the methods used in this study reliably identified the miRNAs.

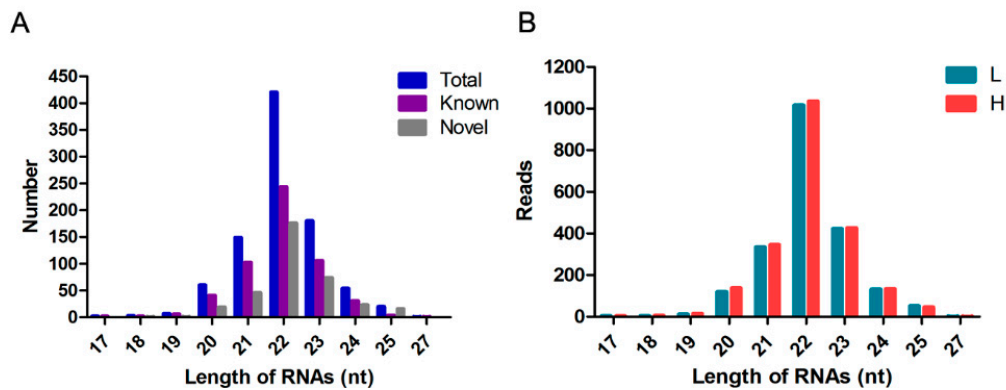


Figure 2. Summary of miRNA-seq data. (A) Distribution of miRNA sequences lengths (total, known, and novel). (B) Distribution of miRNA sequence reads between the H and L groups.

3.3. Identification of Differentially Expressed miRNAs

Of the 24 DE miRNAs identified between the groups, 14 were up-regulated and 10 were down-regulated in the L group relative to the H group (Figure 3A), and of the 24, three were novel miRNAs (Novel_28_448124, Novel_10_52067 and Novel_5_559235) (Table S3). Figure 3B shows the results of a clustering analysis based on the expression profiles for the 24 DE miRNAs. To validate the expression levels, five DE miRNAs were selected and their abundance was measured using qPCR. The results were consistent with those obtained from miRNA deep sequencing (Figure 3C). Among the DE miRNAs, expression of bta-miR-199b was higher in rumen tissue (Table S3). Studies on rumen development in calves indicate that abundance of bta-miR-199b and bta-miR-22-3p change in opposite directions before and after weaning, which is in agreement with the present study [4]. miR-128 [39], miR-127 [40], miR-134 [41], and miR-139 [42] have also been reported to influence the cell proliferation and apoptosis.

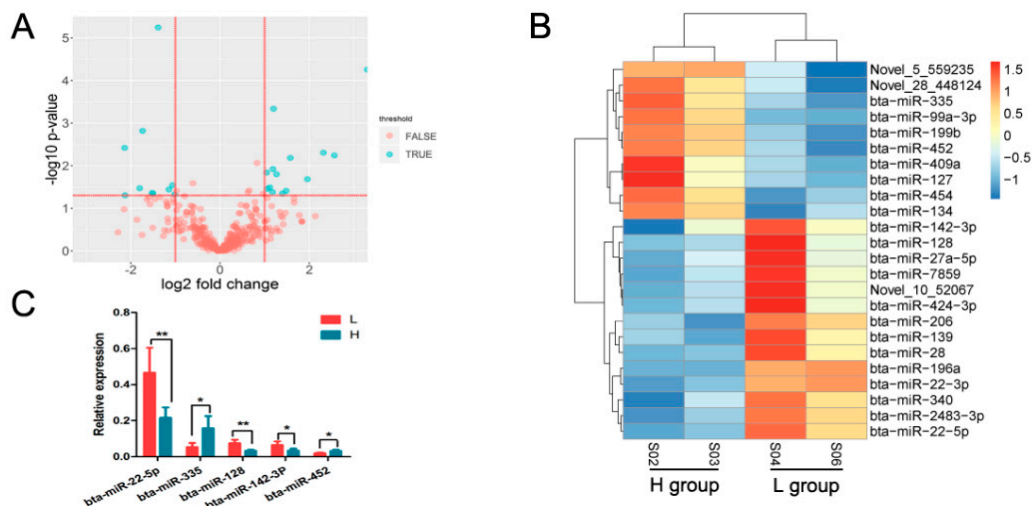


Figure 3. Overview of miRNA deep sequencing data. (A) Volcano plot for differentially expressed miRNAs. (B) Heatmap plot for relative expression abundance of DE miRNAs. (C) Validation of DE miRNAs by qPCR.

3.4. Prediction of DE miRNA Target Genes

To characterize the regulatory roles of the miRNAs in rumen growth and development, target genes were predicted for the DE miRNAs, resulting in 243 potential target genes. bta-miR-127 was associated with the most target genes, followed by bta-miR-139, bta-miR-27a-5p, and bta-miR-134 (Table S3). miRNAs usually suppress protein-encoding mRNAs by complementary binding to the

3'UTR [43]. To validate the negative regulatory relationship between miRNAs and their targets, three DE miRNAs and six target genes (bta-miR-127 with target genes *PYGB*/*COL5A1*, bta-miR-128 with target genes *PPARG*/*SLC16A1*, and bta-miR-139 with target genes *ABCC3*/*PDE5A*) were investigated (Figure 4A–C and Table S4). A negative correlation in expression levels was observed between all miRNAs and their targets. Significant differences were identified between groups, except for the *PYGB* gene. This suggests that the predicted miRNA-target relationships have been verified in this study.

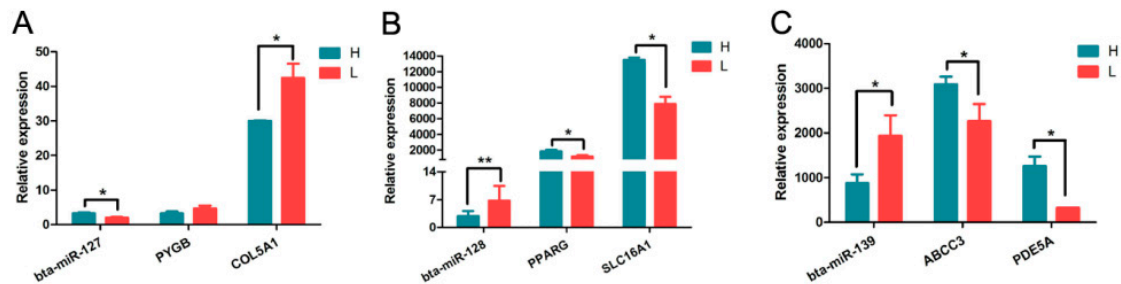


Figure 4. Validation the expression relationship between three DE miRNAs and target genes by qPCR. (A) Relative expression of bta-miR-127 and target genes *PYGB* and *COL5A1*. (B) Relative expression of bta-miR-128 and target genes *PPARG* and *SLC16A1*. (C) Relative expression of bta-miR-139 and target genes *ABCC3* and *PDE5A*.

3.5. Functional Enrichment Analysis

Functional enrichment analysis revealed target genes mainly enriched in regulation of primary metabolic process, single-multicellular organism process, ion binding, DNA binding, and proteinaceous extracellular matrix (Figure 5A and Table S5). The significantly enriched pathways included basal cell carcinoma, ABC transporters, hippo signaling pathway, and calcium signaling pathway (Figure 5B). To better understand the function of the genes of interest in rumen epithelium development, the relationships amongst miRNAs, target genes, and clusters were visualized as an integrated network (Figure 6 and Table S7). The network included DE miRNAs such as bta-miR-127, bta-miR-128, and bta-miR-139, and their target genes. The possible functional role in rumen development of the clusters is discussed below.

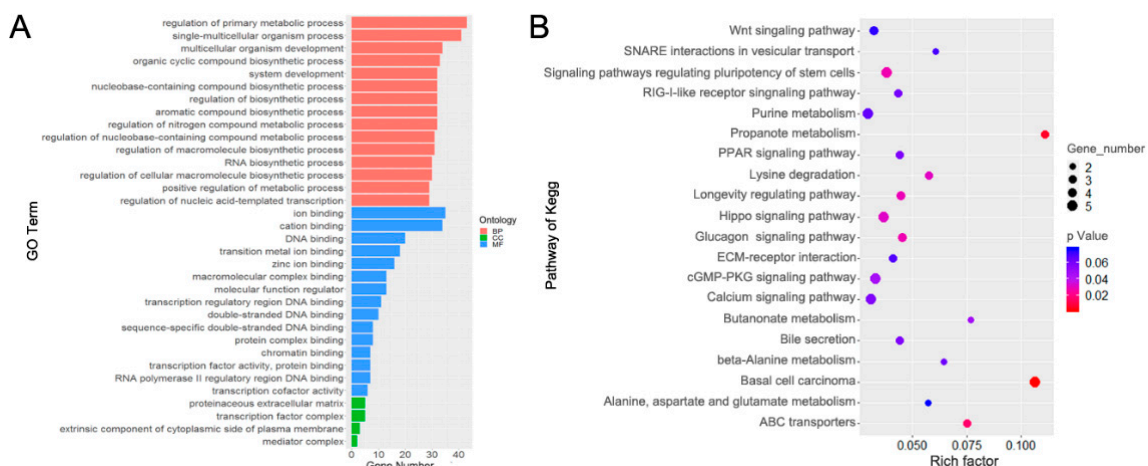


Figure 5. Functional enrichment analyses of DE miRNAs. (A) Gene ontology (GO) enrichment analysis of target genes. Biological process (BP), cellular component (CC), molecular function (MF). (B) Kyoto encyclopedia of genes and genomes (KEGG) pathways enrichment analysis of target genes.

(*ITPR3*) [55], ATPase plasma membrane Ca^{2+} transporting 2 (*ATP2B2*) [56], and ryanodine receptor 1 (*RYR1*) [57], function in the calcium signaling pathway and have a role in cell proliferation and death [58–61] (Table S6). *PPARG* is one of the members of the *PPARs* superfamily [62]. Activation of *PPARG* ligands induced terminal differentiation and apoptosis of keratinocytes and apoptosis in a variety of cell types, including epithelial cancer cell lines [63].

A low NFC/NDF diet is characterized by high fiber and low nutrient levels. Greater amounts of fiber generate more stimulus in rumen epithelium, and this stimulation promotes rumen development [64]. In this study, we found some target genes were enriched in the regulation of extracellular stimuli, namely the KN motif and ankyrin repeat domains 2 (*KANK2*), mediator complex subunit 1 (*MED1*), and peroxisome proliferator activated receptor alpha (*PPARA*) (Figure 6 and Table S5). A high grain content diet can inhibit the growth of rumen papillae because of the lower fiber content of grain. This is consistent with the results of our study, calves fed a diet with less neutral detergent fiber (NDF) had shorter rumen papillae (H group) than calves fed a diet higher in NDF (L group) (Figure 1A). Therefore, the physical stimuli from dietary fiber affects rumen papilla to some extent.

The transport of nutrients is essential for the growth and development of the cells. In this study, some of the target genes were associated with nutritional response cluster, such as *KANK2*, solute carrier family 16 member 1 (*SLC16A1*), and *MED1* (Figure 6 and Table S5). We also found target genes involved in monocarboxylic acid transport, such as *SLC16A1*, TNF superfamily member 11 (*TNFSF11*), HNF1 homeobox A (*HNF1A*), and ATP binding cassette subfamily D member 1 (*ABCD1*) (Figure 6 and Table S5). A large number of studies have shown that short-chain fatty acids produced by fermentation in the rumen are absorbed by rumen cells and metabolizes ketones or lactic acid within the cells or as a source of energy for epithelial cells and most of them were transported to portal vein blood by monocarboxylic acid transporter (*MCT*) [65–67]. *MCT1* (*SLC16A1*) is located at the base of the basal cells in cattle and sheep [68]. The general role of *MCT1* is to take up or release lactic acid from hypoxic-exposed cells, in order to maintain lactate levels during of glycolysis, gluconeogenesis, and lipogenesis [67,69]. Lactic acid can reactivate the tumor microenvironment providing energy for the tumor and thereby promoting its growth [70,71]. In this study, we observed that the relative expression of *SLC16A1* in L group was significantly lower than in the H group (Figure 4B). The accumulation of lactic acid in rumen epithelial cells might promote the development of papillae.

3.6. Targeting Effect of *Bta-miR-128* on *PPARG* and *SLC16A1*

We focused on *bta-miR-128*, which was upregulated in the L group, for a deeper exploration of the biological significance of a candidate DE miRNA. The mature *miR-128* sequence is highly conserved among the various species including pig, zebra finch, human, and mouse (Figure 7A). To identify the direct binding site of *miR-128* on *PPARG* and *SLC16A1*, a 3' UTR fragment of the putative targeting sites with a seed region binding site was inserted into the psiCHECK-2 vector (Figure 7B,C). Luciferase assay revealed that *bta-miR-128* significantly reduced the Rluc activity of the wild-type *PPARG* and *SLC16A1* reporter vector, while point mutations of the seed region of *bta-miR-128* disrupted the suppression (Figure 7B,C). Taken together, these data indicated a negative regulatory relationship between *bta-miR-128* and *PPARG* and *SLC16A1*. *PPARG* and *SLC16A1* are, respectively, involved in cell differentiation and nutritional response processes in the rumen thereby influencing the rumen development. We conclude that *miR-128* is an important miRNA functioning in the rumen development and is affected by NFC/NDF levels.

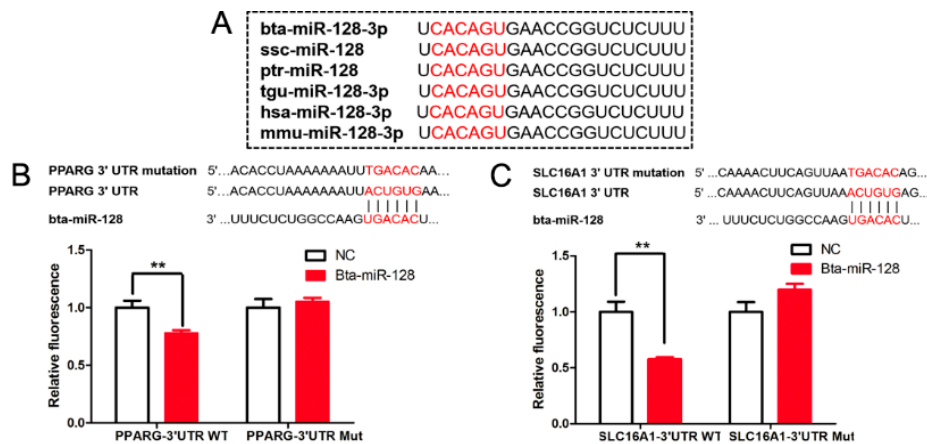


Figure 7. Regulatory effect of bta-miR-128 on PPARG and SLC16A1. (A) Alignment of mature miR-128 sequences from various species. (B) Inhibitory effect of bta-miR-128 on *PPARG* 3'UTR, using the dual-luciferase system. Target site of bta-miR-128 on *PPARG* mRNA 3'UTR and its mutant variant (above) (** $p < 0.01$). (C) Inhibitory effect of bta-miR-128 on *SLC16A1* 3'UTR, using the dual-luciferase system. Target site of bta-miR-128 on *SLC16A1* 3'UTR and its mutant variant (above) (** $p < 0.01$). WT, wild type; Mut, mutant type.

4. Conclusions

In summary, we observed obvious differences in papillae length and width between the rumens of calves fed a diet with high NFC/NDF vs. those fed low NFC/NDF. We have constructed a miRNA-mRNA-cluster network and found through cluster network analysis that cell proliferation, differentiation, physical and nutrient stimuli processes participate in rumen development. In addition, our results suggest that bta-miR-128 is controlled by NFC/NDF levels and may influence the rumen development via regulating PPARG and SLC16A1 expression. Our findings provided evidence for studying the rumen development and absorption.

Supplementary Materials: The following are available online at <http://www.mdpi.com/2076-2615/9/8/496/s1>, Table S1: List of cloning and qPCR primers. Table S2: Descriptive summary of miRNAs reads. Table S3: List of the DE miRNAs identified between H and L rumen tissues. Table S4: Information on target genes of DE miRNAs. Table S5: List of target genes of DE miRNAs enriched in GO categories. Table S6: List of target genes of DE miRNAs enriched in KEGG pathway. Table S7: List of the miRNA-mRNA-cluster network among DE miRNAs, target genes and clusters of interest.

Author Contributions: M.L. and G.S. (Guirong Sun) conceived and designed the experiments. M.X., K.W., A.W., R.L., Y.W., S.S., D.Y., and G.S. (Guohua Song) performed the experiments. M.X. and K.W. analyzed the data. M.X., K.W. and H.X. wrote the paper.

Funding: This research and APC were funded by the Special Fund for the Henan Agriculture Research System (S2013-08-G01).

Conflicts of Interest: The authors declare no conflict of interest.

References

- Wang, B.; Wang, D.; Wu, X.; Cai, J.; Liu, M.; Huang, X.; Wu, J.; Liu, J.; Guan, L. Effects of dietary physical or nutritional factors on morphology of rumen papillae and transcriptome changes in lactating dairy cows based on three different forage-based diets. *BMC Genom.* **2017**, *18*, 353. [CrossRef] [PubMed]
- Li, Y.; Carrillo, J.A.; Ding, Y.; He, Y.; Zhao, C.; Zan, L.; Song, J. Ruminant Transcriptomic Analysis of Grass-Fed and Grain-Fed Angus Beef Cattle. *PLoS ONE* **2015**, *10*, e0116437. [CrossRef] [PubMed]
- Zhong, T.; Hu, J.; Xiao, P.; Zhan, S.; Wang, L.; Guo, J.; Li, L.; Zhang, H.; Niu, L. Identification and Characterization of MicroRNAs in the Goat (*Capra hircus*) Rumen during Embryonic Development. *Front. Genet.* **2017**, *8*, 163. [CrossRef] [PubMed]

4. Do, D.N.; Dudemaine, P.L.; Fomenky, B.E.; Ibeagha-Awemu, E.M. Integration of miRNA weighted gene co-expression network and miRNA-mRNA co-expression analyses reveals potential regulatory functions of miRNAs in calf rumen development. *Genomics* **2019**, *111*, 849–859. [[CrossRef](#)] [[PubMed](#)]
5. Steele, M.A.; Vandervoort, G.; AlZahal, O.; Hook, S.E.; Matthews, J.C.; McBride, B.W. Rumen epithelial adaptation to high-grain diets involves the coordinated regulation of genes involved in cholesterol homeostasis. *Physiol. Genom.* **2011**, *43*, 308–316. [[CrossRef](#)] [[PubMed](#)]
6. Sun, H.Z.; Chen, Y.; Guan, L.L. MicroRNA expression profiles across blood and different tissues in cattle. *Sci. Data* **2019**, *6*, 190013. [[CrossRef](#)] [[PubMed](#)]
7. Li, H.; Wang, Y.; Wu, M.; Li, L.; Jin, C.; Zhang, Q.; Chen, C.; Song, W.; Wang, C. Small RNA Sequencing Reveals Differential miRNA Expression in the Early Development of Broccoli (*Brassica oleracea* var. *italica*) Pollen. *Front. Plant Sci.* **2017**, *8*, 404. [[CrossRef](#)] [[PubMed](#)]
8. Brennecke, J.; Hipfner, D.R.; Stark, A.; Russell, R.B.; Cohen, S.M. Bantam Encodes a Developmentally Regulated microRNA that Controls Cell Proliferation and Regulates the Proapoptotic Gene *hid* in *Drosophila*. *Cell* **2003**, *113*, 25–36. [[CrossRef](#)]
9. Yu, X.; Zhang, L.; Wen, G.; Zhao, H.; Luong, L.A.; Chen, Q.; Huang, Y.; Zhu, J.; Ye, S.; Xu, Q. Upregulated sirtuin 1 by miRNA-34a is required for smooth muscle cell differentiation from pluripotent stem cells. *Cell Death Differ.* **2015**, *22*, 1170–1180. [[CrossRef](#)]
10. Ye, Q.; Zhao, X.; Xu, K.; Li, Q.; Cheng, J.; Gao, Y.; Du, J.; Shi, H.; Zhou, L. Polymorphisms in lipid metabolism related miRNA binding sites and risk of metabolic syndrome. *Gene* **2013**, *528*, 132–138. [[CrossRef](#)]
11. Dragomir, M.P.; Knutsen, E.; Calin, G.A. SnapShot: Unconventional miRNA Functions. *Cell* **2018**, *174*, 1038–1038.e1031. [[CrossRef](#)]
12. Lauressergues, D.; Couzigou, J.M.; Clemente, H.S.; Martinez, Y.; Dunand, C.; Bécard, G.; Combiér, J.P. Primary transcripts of microRNAs encode regulatory peptides. *Nature* **2015**, *520*, 90–93. [[CrossRef](#)]
13. Eiring, A.M.; Harb, J.G.; Neviani, P.; Garton, C.; Oaks, J.J.; Spizzo, R.; Liu, S.; Schwind, S.; Santhanam, R.; Hickey, C.J. miR-328 functions as an RNA decoy to modulate hnRNP E2 regulation of mRNA translation in leukemic blasts. *Cell* **2010**, *140*, 652–665. [[CrossRef](#)]
14. Lehmann, S.M.; Krüger, C.; Park, B.; Derkow, K.; Rosenberger, K.; Baumgart, J.; Trimbuch, T.; Eom, G.; Hinz, M.; Kaul, D. An unconventional role for miRNA: Let-7 activates Toll-like receptor 7 and causes neurodegeneration. *Nat. Neurosci.* **2012**, *15*, 827. [[CrossRef](#)]
15. Tang, R.; Li, L.; Zhu, D.; Hou, D.; Cao, T.; Gu, H.; Zhang, J.; Chen, J.; Zhang, C.Y.; Zen, K. Mouse miRNA-709 directly regulates miRNA-15a/16-1 biogenesis at the posttranscriptional level in the nucleus: Evidence for a microRNA hierarchy system. *Cell Res.* **2012**, *22*, 504–515. [[CrossRef](#)]
16. Lanjie, L.L.; Wang, A.; Lian, H.; Tong, F.U.; Wang, Z.; Diao, Q.; Yan, T.U.; Cheng, S. Effects of diets with different NFC/NDF levels on the growth performance and slaughter performance of meat calves. *J. China Agric. Univ.* **2017**, *22*, 101–109.
17. Van Soest, P.J.; Robertson, J.B.; Lewis, B.A. Methods for Dietary Fiber, Neutral Detergent Fiber, and Nonstarch Polysaccharides in Relation to Animal Nutrition. *J. Dairy Sci.* **1991**, *74*, 3583–3597. [[CrossRef](#)]
18. Mangos, J.A. American journal of physiology. *Am. J. Physiol.* **1917**, *229*, 553–559. [[CrossRef](#)]
19. Carstens, G.E.; Min, B.R.; Pinchak, W.E. Effects of dietary tannin source on performance, feed efficiency, ruminal fermentation, and carcass and non-carcass traits in steers fed a high-grain diet. *Anim. Feed Sci. Technol.* **2010**, *159*, 1–9.
20. Enright, A.J.; Saini, H.K.; van Dongen, S.; Griffiths-Jones, S. miRBase: Tools for microRNA genomics. *Nucleic Acids Res.* **2007**, *36*, D154–D158. [[CrossRef](#)]
21. Friedländer, M.R.; Mackowiak, S.D.; Li, N.; Chen, W.; Rajewsky, N. miRDeep2 accurately identifies known and hundreds of novel microRNA genes in seven animal clades. *Nucleic Acids Res.* **2011**, *40*, 37–52. [[CrossRef](#)]
22. Yang, J.; Zhang, F.; Li, J.; Chen, J.P.; Zhang, H.M. Integrative Analysis of the microRNAome and Transcriptome Illuminates the Response of Susceptible Rice Plants to Rice Stripe Virus. *PLoS ONE* **2016**, *11*, e0146946. [[CrossRef](#)]
23. Wang, L.; Feng, Z.; Wang, X.; Wang, X.; Zhang, X. DEGseq: An R package for identifying differentially expressed genes from RNA-seq data. *Bioinformatics* **2010**, *26*, 136–138. [[CrossRef](#)]
24. Betel, D.; Koppal, A.; Agius, P.; Sander, C.; Leslie, C. Comprehensive modeling of microRNA targets predicts functional non-conserved and non-canonical sites. *Genome Biol.* **2010**, *11*, R90. [[CrossRef](#)]

25. Jan, K.; Marc, R. RNAhybrid: microRNA target prediction easy, fast and flexible. *Nucleic Acids Res.* **2006**, *34*, 451–454.
26. Mao, X.; Cai, T.; Olyarchuk, J.G.; Wei, L. Automated genome annotation and pathway identification using the KEGG Orthology (KO) as a controlled vocabulary. *Bioinformatics* **2005**, *21*, 3787–3793. [[CrossRef](#)]
27. Ashburner, M.; Ball, C.A.; Blake, J.A.; Botstein, D.; Butler, H.; Cherry, J.M.; Davis, A.P.; Dolinski, K.; Dwight, S.S.; Eppig, J.T.; et al. Gene Ontology: Tool for the unification of biology. *Nat. Genet.* **2000**, *25*, 25–29. [[CrossRef](#)]
28. Koonin, E.V.; Fedorova, N.D.; Jackson, J.D.; Jacobs, A.R.; Krylov, D.M.; Makarova, K.S.; Mazumder, R.; Mekhedov, S.L.; Nikolskaya, A.N.; Rao, B.S. A comprehensive evolutionary classification of proteins encoded in complete eukaryotic genomes. *Genome Biol.* **2004**, *5*, R7. [[CrossRef](#)]
29. Saito, R.; Smoot, M.E.; Ono, K.; Ruschinski, J.; Wang, P.L.; Lotia, S.; Pico, A.R.; Bader, G.D.; Ideker, T. A travel guide to Cytoscape plugins. *Nat. Methods* **2012**, *9*, 1069–1076. [[CrossRef](#)]
30. Guo, J.; Zhao, W.; Zhan, S.; Li, L.; Zhong, T.; Wang, L.; Dong, Y.; Zhang, H. Identification and Expression Profiling of miRNAome in Goat longissimus dorsi Muscle from Prenatal Stages to a Neonatal Stage. *PLoS ONE* **2016**, *11*, e0165764. [[CrossRef](#)]
31. Wang, H.; Wang, L.; Wu, Z.; Sun, R.; Jin, H.; Ma, J.; Liu, L.; Ling, R.; Yi, J.; Wang, L.; et al. Three dysregulated microRNAs in serum as novel biomarkers for gastric cancer screening. *Med. Oncol.* **2014**, *31*, 298. [[CrossRef](#)]
32. Khalili, M.; Sadeghizadeh, M.; Ghorbanian, K.; Malekzadeh, R.; Vasei, M.; Mowla, S.J. Down-regulation of miR-302b, an ESC-specific microRNA, in Gastric Adenocarcinoma. *Cell J.* **2012**, *13*, 251–258.
33. Hou, L.; Gu, W.; Zhu, H.; Yao, W.; Wang, W.; Meng, Q. Spiroplasma eriocheiris induces mouse 3T6-Swiss albino cell apoptosis that associated with the infection mechanism. *Mol. Immunol.* **2017**, *91*, 75–85. [[CrossRef](#)]
34. Livak, K.J.; Schmittgen, T.D. Analysis of relative gene expression data using real-time quantitative PCR and the 2⁻(Delta Delta C(T)) Method. *Methods* **2001**, *25*, 402–408. [[CrossRef](#)]
35. Thomas, P.; Smart, T.G. HEK293 cell line: A vehicle for the expression of recombinant proteins. *J. Pharmacol. Toxicol. Methods* **2005**, *51*, 187–200. [[CrossRef](#)]
36. O’Shea, E.; Waters, S.M.; Keogh, K.; Kelly, A.K.; Kenny, D.A. Examination of the molecular control of ruminal epithelial function in response to dietary restriction and subsequent compensatory growth in cattle. *J. Anim. Sci. Biotechnol.* **2016**, *7*, 53. [[CrossRef](#)]
37. Lesmeister, K.E.; Heinrichs, A.J. Effects of corn processing on growth characteristics, rumen development, and rumen parameters in neonatal dairy calves. *J. Dairy Sci.* **2004**, *87*, 3439–3450. [[CrossRef](#)]
38. Steele, M.A.; Croom, J.; Kahler, M.; AlZahal, O.; Hook, S.E.; Plaizier, K.; McBride, B.W. Bovine rumen epithelium undergoes rapid structural adaptations during grain-induced subacute ruminal acidosis. *Am. J. Physiol. Regul. Integr. Comp. Physiol.* **2011**, *300*, R1515–R1523. [[CrossRef](#)]
39. Shi, Z.M.; Wang, J.; Yan, Z.; You, Y.P.; Li, C.Y.; Qian, X.; Yin, Y.; Zhao, P.; Wang, Y.Y.; Wang, X.F. MiR-128 inhibits tumor growth and angiogenesis by targeting p70S6K1. *PLoS ONE* **2012**, *7*, e32709. [[CrossRef](#)]
40. Wang, D.; Tang, L.; Wu, H.; Wang, K.; Gu, D. MiR-127-3p inhibits cell growth and invasiveness by targeting ITGA6 in human osteosarcoma. *IUBMB Life* **2018**, *70*, 411–419. [[CrossRef](#)]
41. Liu, Y.; Zhang, M.; Qian, J.; Bao, M.; Meng, X.; Zhang, S.; Zhang, L.; Zhao, R.; Li, S.; Cao, Q. miR-134 functions as a tumor suppressor in cell proliferation and epithelial-to-mesenchymal Transition by targeting KRAS in renal cell carcinoma cells. *DNA Cell Biol.* **2015**, *34*, 429–436. [[CrossRef](#)]
42. Cui, Y.; Sun, X.; Jin, L.; Yu, G.; Li, Q.; Gao, X.; Ao, J.; Wang, C. MiR-139 suppresses β -casein synthesis and proliferation in bovine mammary epithelial cells by targeting the GHR and IGF1R signaling pathways. *BMC Vet. Res.* **2017**, *13*, 350. [[CrossRef](#)]
43. Shveta, B.; John, B.; Shaun, H.; Katlin, M.; Janette, H.; Rachel, E.; Pasquinelli, A.E. Regulation by let-7 and lin-4 miRNAs results in target mRNA degradation. *Cell* **2005**, *122*, 553–563.
44. Liu, X.G. Histogenesis of the Mongolia Sheep Embryonic Stomach Muscle Layer. *Yinshan Acad. J.* **2004**, *18*, 15–16.
45. Steele, M.A.; Alzahal, O.; Hook, S.E.; Croom, J.; McBride, B.W. Ruminal acidosis and the rapid onset of ruminal parakeratosis in a mature dairy cow: A case report. *Acta Vet. Scand.* **2009**, *51*, 39. [[CrossRef](#)]
46. Greenwood, R.H.; Morrill, J.L.; Titgemeyer, E.C.; Kennedy, G.A. A new method of measuring diet abrasion and its effect on the development of the forestomach. *J. Dairy Sci.* **1997**, *80*, 2534–2541. [[CrossRef](#)]
47. Katoh, M.; Katoh, M. Transcriptional regulation of WNT2B based on the balance of Hedgehog, Notch, BMP and WNT signals. *Int. J. Oncol.* **2009**, *34*, 1411–1415. [[CrossRef](#)]

48. Regl, G.; Neill, G.W.; Eichberger, T.; Kasper, M.; Ikram, M.S.; Koller, J.; Hintner, H.; Quinn, A.G.; Frischauf, A.M.; Aberger, F. Human GLI2 and GLI1 are part of a positive feedback mechanism in Basal Cell Carcinoma. *Oncogene* **2002**, *21*, 5529–5539. [[CrossRef](#)]
49. Watt, K.I.; Harvey, K.F.; Gregorevic, P. Regulation of Tissue Growth by the Mammalian Hippo Signaling Pathway. *Front. Physiol.* **2017**, *8*, 942. [[CrossRef](#)]
50. Oharazawa, H.; Ibaraki, N.; Lin, L.R.; Reddy, V.N. The effects of extracellular matrix on cell attachment, proliferation and migration in a human lens epithelial cell line. *Exp. Eye Res.* **1999**, *69*, 603–610. [[CrossRef](#)]
51. Beharka, A.A.; Nagaraja, T.G.; Morrill, J.L.; Kennedy, G.; Klemm, R.D. Effects of Form of the Diet on Anatomical, Microbial, and Fermentative Development of the Rumen of Neonatal Calves. *J. Dairy Sci.* **1998**, *81*, 1946–1955. [[CrossRef](#)]
52. Zhang, S.Q.; Zan, L.S.; Liang, D.Y.; Gui, L.S. Effect of different dietary concentrate to forage ratio on rumen morphological structure of Chinese Hostein bull. *J. Northwest Agric. For. Univ.* **2009**, *37*, 59–64.
53. Hennings, H.; Michael, D.; Cheng, C.; Steinert, P.; Holbrook, K.; Yuspa, S.H. Calcium regulation of growth and differentiation of mouse epidermal cells in culture. *Cell* **1980**, *19*, 245–254. [[CrossRef](#)]
54. Xie, Z.; Bikle, D.D. Phospholipase C- γ 1 Is Required for Calcium-induced Keratinocyte Differentiation. *J. Biol. Chem.* **1999**, *274*, 20421–20424. [[CrossRef](#)]
55. Weerachayaphorn, J.; Amaya, M.J.; Spirli, C.; Chansela, P.; Mitchellrichards, K.A.; Ananthanarayanan, M.; Nathanson, M.H. Nuclear Factor, Erythroid 2-Like 2 Regulates Expression of Type 3 Inositol 1,4,5-Trisphosphate Receptor and Calcium Signaling in Cholangiocytes. *Gastroenterology* **2015**, *149*, 211–222.e210. [[CrossRef](#)]
56. Minich, R.R.; Li, J.; Tempel, B.L. Early growth response protein 1 regulates promoter activity of α -plasma membrane calcium ATPase 2, a major calcium pump in the brain and auditory system. *BMC Mol. Biol.* **2017**, *18*, 14. [[CrossRef](#)]
57. Hurne, A.; O'Brien, J.; Wingrove, D.; Cherednichenko, G.; Allen, P.; Beam, K.; Pessah, I. Ryanodine receptor type 1 (RyR1) mutations C4958S and C4961S reveal excitation-coupled calcium entry (ECCE) is independent of sarcoplasmic reticulum store depletion. *J. Biol. Chem.* **2005**, *280*, 36994–37004. [[CrossRef](#)]
58. Mikami, Y.; Kanemaru, K.; Okubo, Y.; Nakaune, T.; Suzuki, J.; Shibata, K.; Sugiyama, H.; Koyama, R.; Murayama, T.; Ito, A. Nitric Oxide-induced Activation of the Type 1 Ryanodine Receptor Is Critical for Epileptic Seizure-induced Neuronal Cell Death. *Ebiomedicine* **2016**, *11*, 253–261. [[CrossRef](#)]
59. Pachera, N.; Papin, J.; Zummo, F.P.; Rahier, J.; Mast, J.; Meyerovich, K.; Cardozo, A.K.; Herchuelz, A. Heterozygous inactivation of plasma membrane Ca²⁺-ATPase in mice increases glucose-induced insulin release and beta cell proliferation, mass and viability. *Diabetologia* **2015**, *58*, 2843–2850. [[CrossRef](#)]
60. Blackshaw, S.; Sawa, A.; Sharp, A.H.; Ross, C.A.; Snyder, S.H.; Khan, A.A. Type 3 inositol 1,4,5-trisphosphate receptor modulates cell death. *FASEB J.* **2000**, *14*, 1375–1379. [[CrossRef](#)]
61. Rowther, F.B.; Wei, W.; Dawson, T.P.; Ashton, K.; Singh, A.; Madiessetimchou, M.P.; Thomas, D.G.; Darling, J.L.; Warr, T. Cyclic nucleotide phosphodiesterase-1C (PDE1C) drives cell proliferation, migration and invasion in glioblastoma multiforme cells in vitro. *Mol. Carcinog.* **2016**, *55*, 268–279. [[CrossRef](#)]
62. Burdick, A.D.; Kim, D.J.; Peraza, M.A.; Gonzalez, F.J.; Peters, J.M. The role of peroxisome proliferator-activated receptor- β/δ in epithelial cell growth and differentiation. *Cell. Signal.* **2006**, *18*, 9–20. [[CrossRef](#)]
63. Liliane, M.; Béatrice, D.; Walter, W. Peroxisome-proliferator-activated receptors and cancers: Complex stories. *Nat. Rev. Cancer* **2004**, *4*, 61–70.
64. Norouzian, M.A.; Valizadeh, R. Effect of forage inclusion and particle size in diets of neonatal lambs on performance and rumen development. *J. Anim. Physiol. Anim. Nutr.* **2015**, *98*, 1095–1101. [[CrossRef](#)]
65. Doaa, K.; Junji, M.; Hideaki, H.; Hidetomo, I.; Hiroshi, Y.; Hiroyuki, T.; Seiyu, K. Monocarboxylate transporter 1 (MCT1) plays a direct role in short-chain fatty acids absorption in caprine rumen. *J. Physiol.* **2010**, *576*, 635–647.
66. Kirat, D.; Inoue, H.; Iwano, H.; Hirayama, K.; Yokota, H.; Taniyama, H.; Kato, S. Expression and distribution of monocarboxylate transporter 1 (MCT1) in the gastrointestinal tract of calves. *Res. Vet. Sci.* **2005**, *79*, 45–50. [[CrossRef](#)]
67. Halestrap, A.P.; David, M. The SLC16 gene family—from monocarboxylate transporters (MCTs) to aromatic amino acid transporters and beyond. *Pflügers Arch. Eur. J. Physiol.* **2004**, *447*, 619–628. [[CrossRef](#)]

68. Graham, C.; Gatherar, I.; Haslam, I.; Glanville, M.; Simmons, N.L. Expression and localization of monocarboxylate transporters and sodium/proton exchangers in bovine rumen epithelium. *Am. J. Physiol. Regul. Integr. Comp. Physiol.* **2007**, *292*, R997–R1007. [[CrossRef](#)]
69. Frank, M.; Korinna, H.; Helga, P.; Aschenbach, J.R.R.; Gerhard, B.; Gotthold, G.B. Transport of ketone bodies and lactate in the sheep ruminal epithelium by monocarboxylate transporter 1. *Am. J. Physiol. Gastrointest. Liver Physiol.* **2002**, *283*, G1139.
70. Ippolito, L.; Morandi, A.; Giannoni, E.; Chiarugi, P. Lactate: A Metabolic Driver in the Tumour Landscape. *Trends Biochem. Sci.* **2019**, *44*, 153–166. [[CrossRef](#)]
71. Payen, V.L.; Hsu, M.Y.; Räddecke, K.S.; Wyart, E.; Vazeille, T.; Bouzin, C.; Porporato, P.E.; Sonveaux, P. Monocarboxylate Transporter MCT1 Promotes Tumor Metastasis Independently of Its Activity as a Lactate Transporter. *Cancer Res.* **2017**, *77*, 5591–5601. [[CrossRef](#)]



© 2019 by the authors. Licensee MDPI, Basel, Switzerland. This article is an open access article distributed under the terms and conditions of the Creative Commons Attribution (CC BY) license (<http://creativecommons.org/licenses/by/4.0/>).